

## Controlled Viscosity in Dense Granular Materials

A. Gnoli,<sup>1,2</sup> L. de Arcangelis,<sup>3</sup> F. Giacco,<sup>4</sup> E. Lippiello,<sup>4</sup> M. Pica Ciamarra,<sup>5,6</sup> A. Puglisi,<sup>1,2</sup> and A. Sarracino<sup>1,2</sup>

<sup>1</sup>*Institute for Complex Systems—CNR, Piazzale Aldo Moro 2, 00185 Rome, Italy*

<sup>2</sup>*Department of Physics, University of Rome Sapienza, Piazzale Aldo Moro 2, 00185 Rome, Italy*

<sup>3</sup>*Department of Industrial and Information Engineering, University of Campania “Luigi Vanvitelli,” Aversa (CE) 81031, Italy*

<sup>4</sup>*Department of Mathematics and Physics, University of Campania “Luigi Vanvitelli,” Caserta 81100, Italy*

<sup>5</sup>*CNR-SPIN, Department of Physics, University “Federico II,” Naples, Via Cintia, 80126 Napoli, Italy*

<sup>6</sup>*Division of Physics and Applied Physics, School of Physics and Mathematical Sciences, Nanyang Technological University, 21 Nanyang Link, Singapore 637371, Singapore*



(Received 21 June 2017; revised manuscript received 27 September 2017; published 27 March 2018)

We experimentally investigate the fluidization of a granular material subject to mechanical vibrations by monitoring the angular velocity of a vane suspended in the medium and driven by an external motor. On increasing the frequency, we observe a reentrant transition, as a jammed system first enters a fluidized state, where the vane rotates with high constant velocity, and then returns to a frictional state, where the vane velocity is much lower. While the fluidization frequency is material independent, the viscosity recovery frequency shows a clear dependence on the material that we rationalize by relating this frequency to the balance between dissipative and inertial forces in the system. Molecular dynamics simulations well reproduce the experimental data, confirming the suggested theoretical picture.

DOI: [10.1103/PhysRevLett.120.138001](https://doi.org/10.1103/PhysRevLett.120.138001)

*Introduction.*—Granular systems can be found in solidlike states able to resist applied stresses [1] and in flowing fluidlike states [2,3]. The transition between these regimes is driven by changes in density and in applied stresses, as well as by changes in applied forcing. In this respect, the role of mechanical vibrations [4–32] in driving the unjamming transition is particularly relevant as related to many phenomena, from avalanche dynamics [33] and earthquake triggering [34] in geophysics to the manufacturing process in material, food, and pharmaceutical industries [35]. The influence of applied vibrations on the transition from a solid to a fluidlike state, and possibly from the fluid to the solid state investigated in some numerical simulations [16,36], is an issue of great practical relevance. Indeed, its understanding might open the possibility of controlling the frictional resistance of granular media [19,37,38]. This problem has been addressed by Capozza *et al.* [36,39] on a prototypical model of particles confined between two rigid substrates in relative motion [37,40], the bottom substrates vertically vibrating. Their numerical simulations suggest that viscosity is reduced when the bottom plate vibrates in a range of frequencies, as rationalized through a general argument based on the reduction of effective interface contacts in the system. However, the validity of this argument lacks experimental verification in real granular media.

In this Letter, we experimentally investigate the fluidization properties of different granular materials subject to periodic vertical vibrations in a wide range of frequencies and amplitudes. We probe the viscosity features of the granular system by a vane suspended in it and driven by a motor, see Fig. 1. Measuring the average angular velocity of the vane as

a function of the vibration frequency, we are able to explore a broad range of behaviors of the granular system, from fully jammed to unjammed-fluidized states. Our results confirm the existence of a frequency range in which the system is fluidized, the vane rotating with a finite speed. The transition from the solid to the fluid state occurs at a frequency which is very well estimated by the theory of Ref. [36] that we confirm also investigating particles of different materials. Conversely, we show that the viscosity recovery frequency, where the system transitions from the fluid to the highly viscous state, depends on the material properties. We argue that the material dependence of the viscosity recovery transition originates from a balance condition between dissipative and inertial forces acting in the system, and we support this claim through numerical simulations that allow for precise control of the dissipative forces.

*Experimental setup.*—We study the behavior of a granular system made of  $N = 2600$  spheres, with diameter  $d = 4$  mm, contained in a cylinder with a conical-shaped floor (diameter 90 mm, minimum height 28.5 mm, maximum height 47.5 mm), see Fig. 1, with a packing fraction  $\sim 49$ –52%. The mass of each particle is  $m = 0.267$  g for steel,  $m = 0.0854$  g for glass, and  $m = 0.0462$  g for delrin. The container is vertically vibrated by an electrodynamic shaker (LDS V450) following the protocol:

$$z(t) = A \sin(2\pi ft), \quad (1)$$

where  $z$  is the vertical coordinate of the shaker plate. The maximal acceleration is  $\ddot{z}_{\max} = A(2\pi f)^2$ . The explored frequency and amplitude ranges are 30–700 Hz and

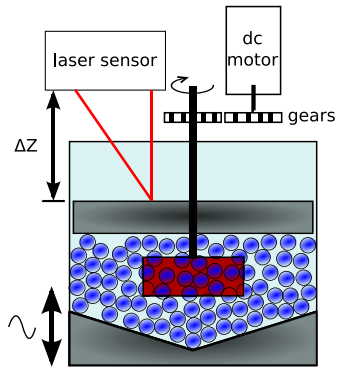


FIG. 1. Experimental setup. A vane (red rectangle) is coupled to a dc motor and is suspended in a dense granular system of spherical particles. The container is vertically vibrated with sinusoidal oscillations of frequency  $f$  and amplitude  $A$ . On the top of the granular medium, there is a plate, whose vertical displacement  $\Delta Z$  is measured with a laser sensor.

0.014–0.053 mm, respectively. Higher values of  $f$  cannot be reached in our setup. Errors on the fixed vibration amplitudes are about 10%. A Plexiglas vane (height 15 mm, width 6 mm, length 35 mm) is suspended in the medium and is subject to an external torque. A dc motor coupled with the rotator is operated at 3 V, producing a torque  $\tau \sim 6 \times 10^{-3}$  N m, see Supplemental Material (SM) [41]. Further details on the experimental setup are given in [30,42,43]. On the top of the granular medium, we place a thick aluminum plate (mass  $M_{\text{top}} = 218$  g). The vertical displacement of the plate  $\Delta Z$  can be measured by a laser device optoNCDT 1400, while the angular position of the vane  $\theta(t)$  is recorded by an encoder.

*Activated fluidization.*—In the absence of vibrations, the applied torque is not able to fluidize the system, which is in a static jammed configuration. We have considered how fluidization occurs when we drive the system, investigating the role of  $f$ , for some fixed values of  $A$ . In Fig. 2 (top panel), we show a typical time dependence of the rotator angular position for different experiments with steel spheres, shaken at  $A = 0.026$  mm. From the signal  $\theta(t)$ , we obtain the average angular velocity  $\omega = \langle d\theta(t)/dt \rangle$ , where the average is taken over trajectories of 30 s. Considering the applied torque constant, the inverse of  $\omega$  is proportional to the macroscopic viscosity of the system. The values of  $\omega$  as a function of  $f$ , for different amplitudes  $A = 0.014, 0.026, 0.053$  mm are reported in the bottom panel of Fig. 2. The behavior of the system, as probed by the rotating vane, is characterized by three regimes. First, at low vibration frequencies, the vane velocity is zero, corresponding to infinite viscosity. This is due to the low energy fed into the system: the granular medium remains at rest in its jammed state, frictionally interacting with the vane. In the second regime, the vane angular velocity rapidly increases and reaches a maximum value  $\omega_{\text{max}}$ . This behavior reflects the jammed-unjammed

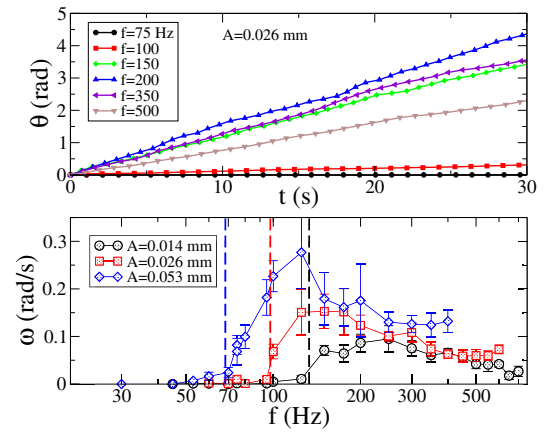


FIG. 2. Top panel: Angular position  $\theta(t)$  of the rotator as a function of time, for different values of  $f$ , at fixed amplitude  $A = 0.026$  mm, for steel spheres. Bottom panel: Average angular velocities  $\omega$  as a function of  $f$  for three shaking amplitudes. The vertical dashed lines represent the theoretical predictions for the fluidization frequencies, see Eq. (2).

transition, induced by the mechanical vibrations, and corresponds to a viscosity reduction in the system. As detailed below, such a fluidized regime corresponds to the detachment condition from the vibrating substrate, where the granular medium expands and the top plate reaches its maximum height. In the third regime, for higher values of  $f$ ,  $\omega$  decreases, signaling an increasing viscosity. Our experimental setup is similar to the one used in [44], where the granular fluid was described as a thermalized system, displaying Brownian motion. In our case, the high density system leads to a more complex phenomenology [42]. Similar studies for granular suspensions are presented in [45,46], where a model predicting their rheology is proposed. However, the dependence on the vibration frequency is not investigated.

The raise of  $\omega$  going from the first to the second regime occurs at a well-defined value of  $f$  that we denote by  $f_1$ . A quantitative estimation of this value can be obtained from the theoretical argument discussed in Refs. [36,39]. Indeed, the fluidization condition is realized when the largest force provided by the shaker  $F = M\ddot{z}_{\text{max}}$ , where  $M$  is the total mass of the system (granular particles and top plate), equals the weight  $Mg$ , with  $g$  being the gravity acceleration. According to this argument, from Eq. (1), the fluidization frequency  $f_1$  is given by the following relation:

$$2\pi f_1 = \sqrt{g/A}. \quad (2)$$

This expression predicts an explicit dependence of the fluidization frequency on the vibration amplitude, very well confirmed by our experimental data, as reported in the bottom panel of Fig. 2 for steel spheres (see vertical dashed lines). In order to demonstrate the generality of the fluidization mechanism, in Fig. 3, we report data obtained in experiments with different materials (steel, glass, and delrin).

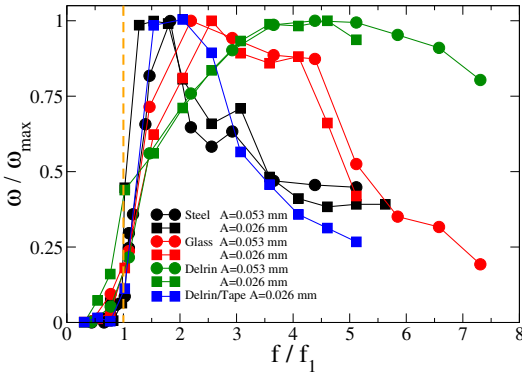


FIG. 3. Rescaled angular velocity, as a function of  $f/f_1$ , for different materials. The vertical dashed line marks the fluidization threshold, according to the theory. Data points are obtained as an average over 10 realizations of the same experiments, with standard deviation  $\sim 15\%$ .

We rescale the frequencies by  $f_1$ , defined in Eq. (2), and  $\omega$  by the maximum value  $\omega_{\max}$  for each data set, obtaining a good collapse of the curves at the onset of the fluidization region. Notice that the activation frequency does not depend significantly on the material, as predicted by Eq. (2). The dependence of  $\omega_{\max}$  on  $A$  is approximately linear, yielding, for steel spheres,  $\omega_{\max} = bA$ , with  $b \simeq 4.66 \text{ s}^{-1} \text{ mm}^{-1}$ , as obtained from data of Fig. 2. Let us note that this fluidization phenomenon is different from the acoustic fluidization mechanism [25,47], related to acoustic waves bouncing back and forth within the medium [48].

The detachment is confirmed by the system dilation for  $f > f_1$ . Further insights are provided by the top plate vertical displacement  $\Delta Z(t)$ . In good agreement with what was observed in the numerical simulations reported in Ref. [36], the power spectrum  $S(\mathcal{F})$  of the signal  $\Delta Z(t)$  shows pronounced peaks at integer multiples of  $f$  for  $f < f_1$ , while in the fluidization region, additional peaks at multiple values of  $f/2$  do appear, see Fig. 4. As already observed in [39], this phenomenology is similar to the problem of period doubling as a route to chaos in the bouncing ball and related models [49,50].

*Viscosity recovery.*—Remarkably, the system exits the state of minimum viscosity at vibration frequencies  $f \gtrsim f_2$ ,

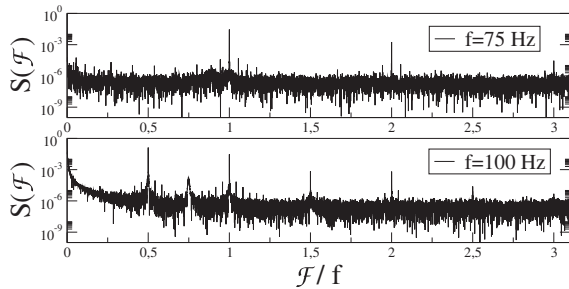


FIG. 4. Power spectrum  $S(\mathcal{F})$  of the signal  $\Delta Z(t)$ , measured in experiments with steel spheres at  $A = 0.026 \text{ mm}$ , in the frictional regime (top panel) and in the fluidized regime (bottom panel).

as shown in Fig. 3. Viscosity recovery at high frequencies has been previously observed in the model system of Ref. [36] and in numerical simulations of a driven spring-block model [16]. According to the argument of Ref. [36], the viscosity recovery is expected to occur when the detachment time from the bottom plate equals the period of the external oscillation. Since in our experiments there is no confining pressure on the top plate and the total normal force is simply  $F_N = Mg$ , the value of  $f_2$  would be proportional to the fluidization frequency  $f_2 = \sqrt{2\pi}f_1$ , without any dependence on the materials. On the contrary, the recovery frequency  $f_2$  observed in our experiments shows a marked dependence on the material:  $\omega$  drops to about  $0.5\omega_{\max}$  at frequencies  $f_2 \sim 3.5f_1$  and  $5f_1$ , for steel and glass, respectively (Fig. 3).

A similar phenomenology is observed in a simple spring-block model under vertical vibration [16]. There, the second transition to a state of larger viscosity originates from a balance between dissipative and inertial forces. More precisely, according to Ref. [16],  $f_2$  depends on the dissipation rate. In our system, this quantity is affected by the elastic and dissipative forces characterizing the grain-grain and grain-interface interactions. To clarify the role of the dissipation at the medium-bottom interface in our system, we performed experiments where the bottom plate is covered with a thick layer of rubber tape, reducing the restitution coefficient in the collisions with the grains. As shown in Fig. 3, the recovery frequency is significantly reduced in this case (compare blue squares to green squares), namely,  $f_2$  decreases upon increasing the dissipation in the system.

*Numerical simulations.*—To confirm the above argument and obtain a quantitative explanation, we have performed molecular dynamics simulations of a granular medium of  $N = 1000$  grains of unitary mass  $m$  and diameter  $d$ , enclosed between two plates. The plates are made of closed packed grains whose relative positions are kept fixed during the dynamics. The system is confined by the gravitational force and has dimensions  $L_x \times L_y = 20d \times 5d$ , with periodic boundary conditions along the  $x$  and  $y$  directions. We use a standard model for the interparticle interaction, see SM for details [41]. The vertical distance  $L_z$  between the plates is not fixed, as the system is allowed to expand under vibration, but typically  $L_z \simeq 10d$ . Data for a larger system size are reported in the SM [41] and show similar behaviors, suggesting that our results are robust and not a finite size effect.

The bottom plate moves according to the same protocol used in the experiments [i.e.,  $z(t) = A \sin(2\pi ft)$ ]. To study the viscous properties of the system, we monitor the motion of a rigid cross-shaped subset of five grains, touching and glued to each other and lying in the plane  $z$ - $y$ . This probe, playing the role of the vane in the experiment, is subject to a constant force  $F$  along the  $x$  direction, while the positions of the five grains are kept fixed along  $z$  and  $y$ . Time is

measured in units of  $t_0$ , and the integration step is  $5 \times 10^{-4} t_0$ . Other parameters are  $F = 500 md/t_0^2$  and  $g = 10 d/t_0^2$ . We employ a contact force model that captures the major features of granular interactions, known as the linear spring-dashpot model, taking into account also the presence of static friction, as fully described in [16,51,52]. Our numerical simulations take into account both normal and tangential frictional forces among grains. We measure the velocity  $v$  of the probe along the  $x$  direction (averaged over trajectories of  $3 \times 10^5 t_0$ ) for different values of  $f$  and  $A$ , chosen in the range  $f \in [10^{-3} t_0^{-1}, 10^{-1} t_0^{-1}]$  and  $A \in [0.05d, 0.2d]$ . Numerical results show a low frequency fluidization transition at  $f_1$  in good agreement with Eq. (2), followed by a viscosity recovery at higher frequencies (Fig. 5). This complex behavior of the velocity is supported by the nonmonotonic behavior of the average particle coordination number, shown in the SM [41]. A similar behavior of this quantity is also observed in the range of frequencies of acoustic fluidization [53].

These results, combined with the analysis of translational and rotational kinetic energies (see SM [41]), indicate that in the high frequency regime, the system attains high density values, and a relevant fraction of kinetic energy is rotational, in agreement with Refs. [54,55], for systems under shear. In the following, we focus on the viscosity recovery transition observed at higher frequencies whose behavior is expected to depend on the dissipation mechanisms.

In numerical simulations, we can change the viscoelastic properties of the system by tuning the rigidity of each grain, corresponding to a change in the restitution coefficient of each grain  $e$  [51]. Frictional dissipation can be neglected, see SM [41]. More precisely, to reproduce the experimental

setup, we consider two different restitution coefficients:  $e_g$  for grain-grain collisions and  $e_b$  for collisions between grain and bottom plate. In Fig. 5, we show the value of  $v/v_{\max}$  as a function of  $f/f_1$  for different values of  $e_g$  and  $e_b$ . Results clearly indicate that  $f_1$  is not affected by  $e_b$  and  $e_g$ , whereas the recovery frequency  $f_2$  depends on the dissipation. In particular, we expect that the smaller is the fraction of energy lost in a collision, the higher is the value of the recovery frequency  $f_2$ , since the system needs a larger number of collisions to dissipate the amount of energy necessary for the viscosity recovery. More specifically, the rate of energy dissipation can be estimated as  $(1 - e^2)f$  [56] (the main assumption here being that the collision frequency is  $\propto f$ ), giving a condition for the viscosity recovery of the kind  $(1 - e^2)f_2 > \text{const}$ . To verify this dependence of  $f_2$  on  $e$ , we consider the simplest case  $e = e_g = e_b$  and define  $f_2$  as the value of the shaking frequency for which the velocity of the probe is  $v = 0.25 v_{\max}$ . From the results reported in the inset of Fig. 5, we obtain a behavior  $f_2/f_1 \sim (1 - e^2)^{-1}$ , in agreement with the above argument. As in the experiments, these findings are not consistent with the scenario of [36], where the frequency  $f_2$  is related to the rise time associated with the internal vibrations of the grains. Our numerical results also indicate that the main dissipation in the system occurs at the medium-bottom interface, as illustrated in Fig. 5, where black and green symbols correspond to sets with  $e_b$  and  $e_g$  values interchanged. This scenario is confirmed by the direct measurement of the energy dissipated in the bulk and at the bottom interface, see SM [41]. Note that in the simulations we did not consider a dependence of the restitution coefficient on the impact velocity. Since the collision velocity changes with the vibration frequency, the restitution coefficient could increase up to 30%, depending on the material parameters [57–60]. This could explain some differences between the experimental and numerical curves.

*Conclusion.*—We have studied experimentally the viscous properties of dense granular materials under vertical vibration. Using a vane subject to an external torque as the probe, we have observed different regimes in the system, from very large viscosity at low vibration frequencies to fluidized states (corresponding to viscosity reduction) at intermediate  $f$ , with a viscosity recovery at higher values of  $f$ . The first transition to the fluidized state is well characterized by the detachment condition and is independent of the material properties. The second transition, leading to viscosity recovery, turns out to be related to dissipation mechanisms in the medium and between the medium and the bottom plate and therefore shows a strong dependence on materials. Our study suggests the possibility to control the viscous properties of confined granular media by tuning the shaking frequency in the system, with important practical application in several fields, from tribology to geophysics and the material industry.

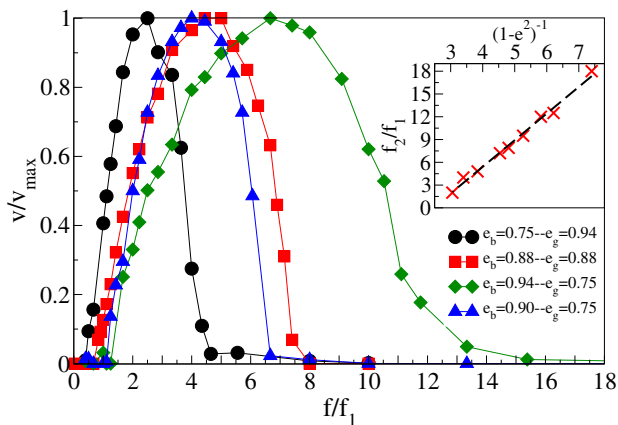


FIG. 5. Numerical simulations. Rescaled velocity of the probe as a function of  $f/f_1$ . Data are obtained for systems with different values of  $e_g$  and  $e_b$ , chosen in analogy with the experiments (see Fig. 3). Inset: The rescaled values of the recovery frequency  $f_2$  as a function of the inverse of the dissipation factor  $1 - e^2$  for systems with  $e_g = e_b$ .

- [1] H. M. Jaeger, S. R. Nagel, and R. P. Behringer, *Rev. Mod. Phys.* **68**, 1259 (1996).
- [2] N. V. Brilliantov and T. Pöschel, *Kinetic Theory of Granular Gases* (Oxford University Press, New York, 2004).
- [3] A. Puglisi, *Transport and Fluctuations in Granular Fluids* (Springer, New York, 2015).
- [4] É. Falcon, S. Fauve, and C. Laroche, *Eur. Phys. J. B* **9**, 183 (1999).
- [5] M. Urbakh, J. Klafter, D. Gourdon, and J. Israelachvili, *Nature (London)* **430**, 525 (2004).
- [6] C. Huan, X. Yang, D. Candela, R. W. Mair, and R. L. Walsworth, *Phys. Rev. E* **69**, 041302 (2004).
- [7] P. A. Johnson and X. Jia, *Nature (London)* **437**, 871 (2005).
- [8] K. E. Daniels and R. P. Behringer, *Phys. Rev. Lett.* **94**, 168001 (2005).
- [9] M. Pica Ciamarra, A. Coniglio, and D. De Martino, *Eur. Phys. J. E* **24**, 411 (2007).
- [10] T. Brunet, X. Jia, and P. A. Johnson, *Geophys. Res. Lett.* **35**, L19308 (2008).
- [11] P. A. Johnson, H. Savage, M. Knuth, J. Gombert, and C. Marone, *Nature (London)* **451**, 57 (2008).
- [12] Ph. Marchal, N. Smirani, and L. Choplin, *J. Rheol.* **53**, 1 (2009).
- [13] M. Griffa, E. G. Daub, R. A. Guyer, P. A. Johnson, C. Marone, and J. Carmeliet, *Europhys. Lett.* **96**, 14001 (2011).
- [14] A. L. Sellerio, D. Mari, G. Gremaud, and G. D'Anna, *Phys. Rev. E* **83**, 021301 (2011).
- [15] J. A. Dijksman, G. H. Wortel, L. T. H. van Dellen, O. Dauchot, and M. van Hecke, *Phys. Rev. Lett.* **107**, 108303 (2011).
- [16] F. Giacco, E. Lippiello, and M. Pica Ciamarra, *Phys. Rev. E* **86**, 016110 (2012).
- [17] J. N. van der Elst, E. E. Brodsky, P. Y. Le Bas, and P. A. Johnson, *J. Geophys. Res.* **117**, B09314 (2012).
- [18] P. A. Johnson, B. M. Carpenter, M. Knuth, B. M. Kaproth, P. Y. Le Bas, E. G. Daub, and C. Marone, *J. Geophys. Res.* **117**, B04310 (2012).
- [19] J. Krim, *Adv. Phys.* **61**, 155 (2012).
- [20] M. Pica Ciamarra, F. Dalton, L. de Arcangelis, C. Godano, E. Lippiello, and A. Petri, *Tribol. Lett.* **48**, 89 (2012).
- [21] M. Griffa, B. Ferdowsi, R. A. Guyer, E. G. Daub, P. A. Johnson, C. Marone, and J. Carmeliet, *Phys. Rev. E* **87**, 012205 (2013).
- [22] B. Ferdowsi, M. Griffa, R. A. Guyer, P. A. Johnson, C. Marone, and J. Carmeliet, *Geophys. Res. Lett.* **40**, 4194 (2013).
- [23] B. Ferdowsi, M. Griffa, R. A. Guyer, P. A. Johnson, C. Marone, and J. Carmeliet, *Phys. Rev. E* **89**, 042204 (2014).
- [24] B. A. Klumov, Y. Jin, and H. A. Makse, *J. Phys. Chem. B* **118**, 10761 (2014).
- [25] F. Giacco, L. Saggese, L. de Arcangelis, E. Lippiello, and M. P. Ciamarra, *Phys. Rev. Lett.* **115**, 128001 (2015).
- [26] P. Charbonneau, E. I. Corwin, G. Parisi, and F. Zamponi, *Phys. Rev. Lett.* **114**, 125504 (2015).
- [27] H. Lastakowski, J.-C. Géminard, and V. Vidal, *Sci. Rep.* **5**, 13455 (2015).
- [28] A. Pons, A. Amon, T. Darnige, J. Crassous, and E. Clément, *Phys. Rev. E* **92**, 020201(R) (2015).
- [29] M. Bouzid, A. Izzet, M. Trulsson, E. Clément, P. Claudin, and B. Andreotti, *Eur. Phys. J. E* **38**, 125 (2015).
- [30] A. Gnoli, A. Lasanta, A. Sarracino, and A. Puglisi, *Sci. Rep.* **6**, 38604 (2016).
- [31] G. Wortel, O. Dauchot, and M. van Hecke, *Phys. Rev. Lett.* **117**, 198002 (2016).
- [32] F. Santibanez, R. Zuniga, and F. Melo, *Phys. Rev. E* **93**, 012908 (2016).
- [33] *Physics of Dry Granular Media*, edited by H. J. Herrmann, J.-P. Hovi, and S. Luding (Springer Science & Business Media, New York, 2013), Vol. 350.
- [34] L. de Arcangelis, C. Godano, J. R. Grasso, and E. Lippiello, *Phys. Rep.* **628**, 1 (2016).
- [35] P. Coussot, *Rheometry of Pastes, Suspensions, and Granular Materials: Applications in Industry and Environment* (John Wiley & Sons, New York, 2005).
- [36] R. Capozza, A. Vanossi, A. Vezzani, and S. Zapperi, *Phys. Rev. Lett.* **103**, 085502 (2009).
- [37] B. Persson, *Sliding Friction: Physical Principles and Applications* (Springer Science & Business Media, New York, 2013).
- [38] A. Vanossi, N. Manini, M. Urbakh, S. Zapperi, and E. Tosatti, *Rev. Mod. Phys.* **85**, 529 (2013).
- [39] R. Capozza, A. Vanossi, A. Vezzani, and S. Zapperi, *Tribol. Lett.* **48**, 95 (2012).
- [40] O. M. Braun and M. Peyrard, *Phys. Rev. E* **63**, 046110 (2001).
- [41] See Supplemental Material at <http://link.aps.org/supplemental/10.1103/PhysRevLett.120.138001> for additional numerical data.
- [42] A. Gnoli, A. Puglisi, A. Sarracino, and A. Vulpiani, *PLoS One* **9**, e93720 (2014).
- [43] C. Scalliet, A. Gnoli, A. Puglisi, and A. Vulpiani, *Phys. Rev. Lett.* **114**, 198001 (2015).
- [44] G. D'Anna, P. Mayor, A. Barrat, V. Loreto, and F. Nori, *Nature (London)* **424**, 909 (2003).
- [45] C. Hanotin, S. K. de Richter, P. Marchal, L. J. Michot, and C. Baravian, *Phys. Rev. Lett.* **108**, 198301 (2012).
- [46] C. Hanotin and S. K. de Richter, *J. Rheol.* **59**, 253 (2015).
- [47] H. J. Melosh, *Nature (London)* **379**, 601 (1996).
- [48] Assuming a sound velocity of the order of 600 m/s for a dense granular medium of glass beads [7], we expect a resonant frequency at roughly 50 kHz.
- [49] J. M. Luck and A. Mehta, *Phys. Rev. E* **48**, 3988 (1993).
- [50] A. S. de Wijn and H. Kantz, *Phys. Rev. E* **75**, 046214 (2007).
- [51] L. E. Silbert, D. Ertaş, G. S. Grest, T. C. Halsey, D. Levine, and S. J. Plimpton, *Phys. Rev. E* **64**, 051302 (2001).
- [52] P. A. Cundall and O. D. L. Strack, *Geotechnique* **29**, 47 (1979).
- [53] C. J. Olson Reichhardt, L. M. Lopatina, X. Jia, and P. A. Johnson, *Phys. Rev. E* **92**, 022203 (2015).
- [54] O. Dorostkar, R. A. Guyer, P. A. Johnson, C. Marone, and J. Carmeliet, *J. Geophys. Res. Solid Earth* **122**, 3689 (2017).

- [55] B. Ferdowsi, M. Griffa, R. A. Guyer, P. A. Johnson, C. Marone, and J. Carmeliet, *Geophys. Res. Lett.* **42**, 9750 (2015).
- [56] V. Kumaran, *Phys. Rev. E* **57**, 5660 (1998).
- [57] G. Kuwabara and K. Kono, *Jpn. J. Appl. Phys.* **26**, 1230 (1987).
- [58] N. V. Brilliantov, F. Spahn, J.-M. Hertzsch, and T. Pöschel, *Phys. Rev. E* **53**, 5382 (1996).
- [59] R. Ramírez, T. Pöschel, N. V. Brilliantov, and T. Schwager, *Phys. Rev. E* **60**, 4465 (1999).
- [60] S. McNamara and E. Falcon, *Phys. Rev. E* **71**, 031302 (2005).